Superposition Modulation-Based Cooperation for Oversampled OFDM Signals

Alireza Rahmati, Kaamran Raahemifar, *Senior Member, IEEE*, Alagan Anpalagan, *Senior Member, IEEE*, Theodoros A. Tsiftsis, *Senior Member, IEEE*, Paeiz Azmi, *Senior Member, IEEE*, and Nikolaos I. Miridakis

***Abstract*— This paper proposes an iterative detector for uncoded OFDM signals in cooperative networks, where the information symbols are simply partitioned through a time-domain matrix at the OFDM transmitter. We analytically show that our proposed iterative detector at the partner node converges and can completely recover the user's data from its partitioned version, if sufficient redundancy is inserted in the user's data. For efficient use of the redundancy in the user's data, a coded cooperative transmission based on superposition modulation is proposed. Additionally, a closed-form input–output relationship for the partitioning and reconstruction algorithm in the proposed cooperative scenario is derived. We also obtain closed-form expressions for symbol error rate performance of the proposed coded cooperative scenario over Rayleigh frequency-selective fading channels. Numerical comparisons shed light on the relative merits of the proposed coded cooperation under various inter-user and uplink channel conditions.**

***Index Terms*— Coded cooperative diversity, iterative detection, orthogonal frequency division multiplexing (OFDM) systems.**

I. INTRODUCTION

USER cooperation diversity has already emerged as a new form of spatial diversity whereby diversity gains are attained via cooperation of sparse terminals in wireless networks, although each of them is equipped with only one antenna [1]. On the other hand, in the modern wireless communication, OFDM technology has become an integral part of the communications standards, such as 802.11n/ac, 802.16, and 4G. A number of benefits the OFDM brings to cooperative relay systems originate from the basic features that it possesses.

Manuscript received February 2, 2017; revised May 15, 2017; accepted July 5, 2017. Date of publication July 17, 2017; date of current version November 15, 2017. This work was supported in part by the National Science and Engineering Research Council of Canada through Discovery Grant and in part by ENGAGE Grant. The associate editor coordinating the review of this paper and approving it for publication was A. Tajer. *(Corresponding author: Theodoros A. Tsiftsis.)*

A. Rahmati, K. Raahemifar, and A. Anpalagan are with the Department of Electrical and Computer Engineering, Ryerson University, Toronto, M5B 2K3 ON, Canada (e-mail: alireza.rahmati@ryerson.ca; kraahemi@ee.ryerson.ca; alagan@ee.ryerson.ca).

T. A. Tsiftsis is with the School of Engineering, Nazarbayev University, Astana 010000, Kazakhstan (e-mail: theodoros.tsiftsis@nu.edu.kz).

P. Azmi is with the Department of Electrical and Computer Engineering, Tarbiat Modares University, Tehran 14115-194, Iran (e-mail: pazmi@modares.ac.ir).

N. I. Miridakis is with the Department of Computer Engineering, Piraeus University of Applied Sciences, 122 44 Aegaleo, Greece (e-mail: nikozm@unipi.gr).

Color versions of one or more of the figures in this paper are available online at http://ieeexplore.ieee.org.

Digital Object Identifier 10.1109/TCOMM.2017.2727497

A. Literature Review and Motivation

In place of repetition based cooperative schemes, e.g. amplify-and-forward (AF) [2]–[4] and decode-and-forward (DF) [5]–[7], coded cooperation has been recently proposed for its efficient usage of the available bandwidth and its ability to adapt to channel conditions through varying its coding rate [8], [9]. The key characteristic of this scheme is that cooperation, which is integrated with channel coding [10], occurs through partitioning a user's codeword such that a part of the codeword is transmitted by the user itself, while the remainder is transmitted by the partner through partial or complete decoding. Several distributed coding schemes have been proposed for coded cooperation and codeword partitioning, including convolutional codes [11], distributed space-time coding [12], [13], distributed low density parity check codes [14] as well as distributed turbo coding schemes [15]. A more efficient transmission scheme based on superposition modulation was first proposed in [16], where for each user, the overheard information from its partner is processed and superimposed onto its own information for cooperative transmission over Rayleigh flat fading channels. To reap both reliability and throughput benefits in frequency-selective fading environment, the cooperative OFDM system has been widely studied recently [17], [18]. Although the information-theoretic analysis of the superposition modulation-based cooperation in [16] has been reported in [19]–[21], only limited work on the design of practical schemes for OFDM systems can be found in the literature. For instance, DF cooperative OFDM system with signal space diversity, a modified version of the superposition modulation-based cooperation obtained through constellation rotation, was introduced in [22]. To the best of the authors' knowledge, the first implementation of the coded cooperative OFDM system based on superposition modulation has been proposed in [23]; however, in this paper no analytical results have been given with respect to the iterative detection method and the error rate performance for this user-cooperation strategy. Furthermore, the flat fading channel environment that is strange for OFDM practical applications has been considered for simplicity in [23].

B. Contributions

In this paper, a coded cooperative scenario for uncoded OFDM systems is investigated, where user's data partitioning is provided through the puncturing matrix, instead of using extra channel coding employed in conventional coded cooperation. We also analytically prove that the partner node can completely recover the user's data from its punctured version through an iterative reconstruction algorithm, if sufficient redundancy is increased in each user's OFDM block. Increased redundancy, which causes the iterative reconstruction algorithm to converge in the proposed coded cooperative communication, is applied via the oversampling potential in OFDM without the requirement of using extra channel coding. This can potentially save more bandwidth for the transmission. Moreover, using extra channel coding as in convolutional coded cooperative systems may call for very long interleaving and the complex Viterbi decoding algorithm. Oversampling in OFDM [24], a special case of redundant precoding in OFDM [25]–[28], is realized by padding the modulating sequence with some zeros before taking IFFT at the transmitter. This can be used for providing other properties as well, such as decreasing edge effects of OFDM signal in frequency domain, mitigating intersymbol interference (ISI), channel estimation, and PAPR (Peak-to-Average Power Ratio) reduction [29], [30]. Although the oversampling potential in OFDM decreases the bandwidth efficiency due to zero symbols transmission, we show that the user node can employ these known idle subcarriers for transmitting a segment of the partner node's data. Thereby, the proposed coded cooperative system is derived as a direct result of oversampling, which is based on superposition transmission which efficiently uses the extended bandwidth. Specifically, the contributions of this paper are as follows:

- A perfect recovery method through nonlinear but simple and fast converging iterative method for oversampled OFDM signals in coded cooperation is proposed.
- The closed-form input-output relationship of the coded cooperation for oversampled OFDM signals is obtained. Also, the recovered signal model at the partner node for arbitrary number of iteration is derived.
- A precise method for calculating the symbol error rate (SER) of the coded cooperation for oversampled OFDM signals is presented.
- A simple puncturing method for partitioning user's data packets in coded cooperation and superposition modulation based cooperation for oversampled OFDM signals is devised.
- Convergence condition for iterative reconstruction of OFDM samples is obtained. We theoretically proved that convergence of proposed iterative method depends on the eigenvalues of the puncturing operator.
- Computational complexity of iterative reconstruction of OFDM samples for an arbitrary number of iteration is derived.
- We obtained the minimum sampling rate needed for errorless transmission, and the relationship between the sampling rate and the cooperation level is extracted.
- Simulation results are given to support our theoretical analyses and to show that with a lower decoding and implementation complexity, our proposed scheme can achieve better performance than the Bose, Chaudhuri, and Hocquenghem (BCH), Reed-Solomon (RS), and low density parity check (LDPC) coded OFDM schemes over erasure channels.

TABLE I

VARIABLES AND THEIR DESCRIPTIONS

Variable	Description
$\mathbf{G}_t$	Diagonal puncturing matrix
$\mathbf{h}$	Channel impulse response vector
L	Channel memory length
$\mathbf{c}'$	Transmit vector of modulated bits
$\mathbf{s}$	Punctured version of IFFT (inverse fast Fourier transform) of $\mathbf{c}'$
$\mathbf{r}$	Received vector after FFT (fast Fourier transform)
ν	White Gaussian noise vector with zero mean and variance N_0
$\mathbf{H}$	$N \times N$ Circulant channel matrix with $[\mathbf{H}]_{ij} = h((i-j)\ mod\ N)$
$\mathbf{\Psi}$	Uniform sampled version of received vector

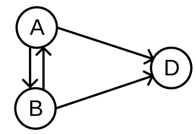

Fig. 1. Basic cooperation system model.

The rest of the paper is organized as follows. In Section II the proposed coded cooperative transmission scheme for OFDM systems, which uses the time domain puncturing matrix for partitioning the userâŁ™s data, is described. An iterative reconstruction method for complete recovery of userâŁ™s data at the partner node is also explained in this section. Coded cooperative diversity based on superposition modulation for oversampled OFDM signals is described in Section III. Simulation results are presented and discussed in Section IV, and concluding remarks are presented in Section V. *Notation:* Superscripts ^{T}, ^{H}, and † denote transposition, conjugate transposition, and Moore-Penrose matrix inversion, respectively. $E\{\cdot\}$ denotes statistical expectation. $[\cdot]_{i,j}$ denotes the (i, j)th entry of a matrix. diag$\{\mathbf{x}\}$ is a diagonal matrix with $\mathbf{x}$ on its main diagonal. $\mathbf{I}_N$ is the $N \times N$ identity matrix. $\mathbf{0}_{M \times N}$ denotes an M-by-N all-zero matrix. $\|\mathbf{x}\|$ denotes the norm of vector $\mathbf{x}$. The ith element of vector $\mathbf{x}$ is denoted by $\mathbf{x}(i)$. $\mathcal{CN}(\mu, \sigma^2)$ denotes the complex Gaussian distribution with mean μ and variance σ^2, whereas $\mathcal{N}(\mu, \sigma^2)$ denotes the real Gaussian distribution with mean μ and variance σ^2. Real and imaginary parts are denoted by Re(.) and Im(.). The kth column and kth row vectors of matrix $\mathbf{X}$ are denoted by $\mathbf{X}(:, k)$ and $\mathbf{X}(k, :)$, respectively. $\mathbf{F}_N$ denotes the normalized $N \times N$ discrete Fourier transform (DFT) matrix whose $(n+1, k+1)$th entry is exp $(-j2\pi nk/N)/\sqrt{N}$ (Also, see Table I).

II. CODED COOPERATIVE DIVERSITY FOR OFDM SYSTEMS

A. System Model

The OFDM coded cooperative network over multipath fading channels is considered in Fig. 1. Two source nodes, A and B, are paired as partners for transmission of their data to a common destination node, D. All terminals are equipped with a single transmit and receive antenna. It is assumed that the half-duplex mode of operation (either transmit or receive, but not both) is imposed on the cooperating nodes. The

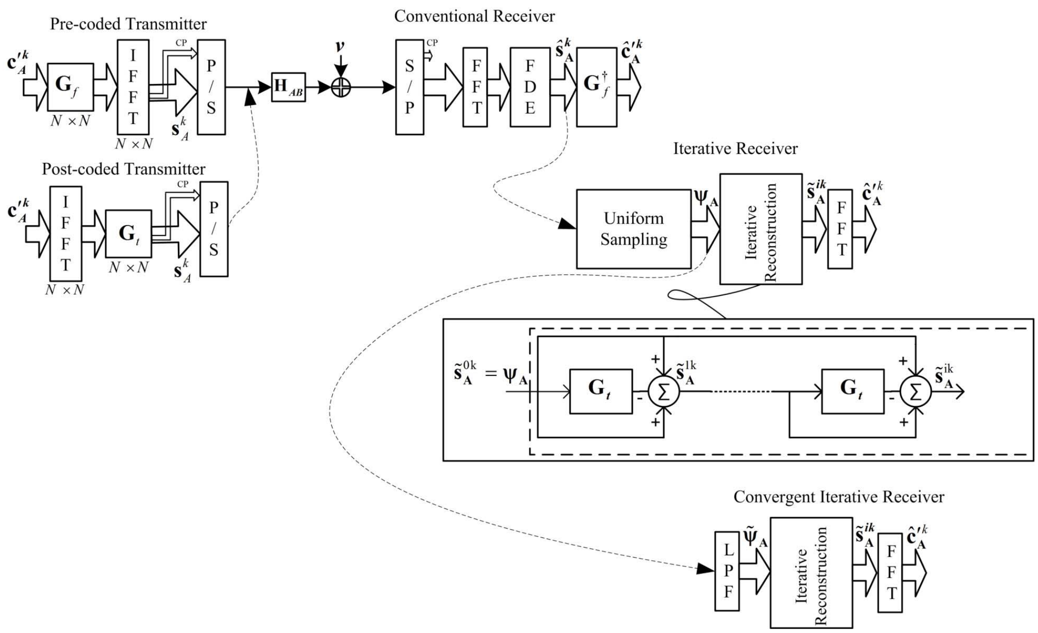

Fig. 2. Node A in cooperation step k as a post-coded OFDM and its equivalent pre-coded OFDM system at the transmit side. The conventional, the iterative and the convergent iterative schemes at node Node B in cooperation step k.

channel impulse responses (CIRs) for the A $\rightarrow$ B, B $\rightarrow$ A, A $\rightarrow$ D, and B $\rightarrow$ D links for each transmission block are given by $\mathbf{h_{AB}} = \mathbf{h_{BA}} = [h_{AB}(0),\ h_{AB}(1),\ \ldots,\ h_{AB}(L_{AB})]^T$, $\mathbf{h_{AD}} = [h_{AD}(0),\ h_{AD}(1),\ \ldots,\ h_{AD}(L_{AD})]^T$, and $\mathbf{h_{BD}} = [h_{BD}(0),\ h_{BD}(1),\ \ldots,\ h_{BD}(L_{BD})]^T$, respectively, where $L_{AB} = L_{BA}$, L_{AD}, and L_{BD} denote the corresponding channel memory lengths. Note that the channel between nodes A and B is assumed to be a reciprocal channel. Node A transmits a part of its data in step k and node B transmits other part of node A's data in step $k+1$. To transmit a part of node A's data in the proposed cooperative scenario, a simple diagonal puncturing matrix of $\mathbf{G}_t = \mathrm{diag}(g_{t1}, \ldots, g_{tN})$, $g_{tm} \in \{0, 1\}$ is inserted after the IFFT transform at the transmit side of node A. To clarify how a part of node A's data is transmitted in cooperation step k, see the transmitter in Fig. 2 where information symbols $c'^{k}_{A}(m)$ are 2^Q- phase-shift keying (PSK) or 2^Q- quadrature amplitude modulation (QAM) modulated, in which Q is the number of bits per symbol, and are segmented into blocks with size N to provide node A's total data $\mathbf{c'^k_A} = [c'^k_A(1),\ c'^k_A(2),\ \ldots,\ c'^k_A(N)]^T$. Then, $\mathbf{c'^k_A}$ is punctured with block of $\mathbf{G}_t$ to provide node A's data in cooperation step k, $\mathbf{s^k_A}$. It should be stated that conventional coded cooperative schemes employ some form of channel coding to segment the user's data. As an example, see a coded cooperation with rate compatible punctured convolutional (RCPC) code described in [31]. In our proposed cooperative scenario, the remaining data of node A is easily transmitted by the puncturing matrix of $\mathbf{I}_N - \mathbf{G}_t$ at node B in step $k+1$ where $\mathbf{I}_N$ is identity matrix of size N. Note that the channel states and the puncturing matrix $\mathbf{G}_t$ are known at all nodes in our system model. Henceforth, we show how the $\mathbf{G}_t$ can be modelled in conventional OFDM system by applying the matrices of $\mathbf{G}_t$ and $\mathbf{I}_N - \mathbf{G}_t$ in time domain, and a postcoded OFDM [32] in both of the A and B nodes is implemented. It can easily be shown that any postcoding scheme can be made equivalent to a precoding scheme by selecting

$$\left.\begin{aligned} \mathbf{s^k_A} &= \mathbf{G}_t \mathbf{F}_N^H \mathbf{c'^k_A} \\ \mathbf{s^k_A} &= \mathbf{F}_N^H \mathbf{G}_f \mathbf{c'^k_A} \end{aligned}\right\} \Rightarrow \mathbf{G}_f = \mathbf{F}_N \mathbf{G}_t \mathbf{F}_N^H. \tag{1}$$

Fig. 2 shows the postcoded and its equivalent precoded OFDM transmitter for node A. It can be easily seen that the equivalent precoding scheme for node B in step $k+1$ is $\mathbf{I}_N - \mathbf{G}_f$. To remove inter block interference and make the channel matrix circulant, a cyclic prefix (CP) with length $l_A = \max\ (L_{AB},\ L_{AD})$ and $l_B = \max\ (L_{BA},\ L_{BD})$ is added between adjacent information blocks at node A and node B, respectively. Note that the postcoder of $\mathbf{G}_t$ discards some part of node A's data and it has no impact on frequency-selectivity effects of the channel. Thus, in a similar manner as in many precoded OFDM systems employing the frequency domain equalizer, e.g. [33], by cyclic prefix insertion with duration no shorter than the channel order among transmitting data, $\mathbf{s^k_A}$, frequency-selective fading channel turns into a set of parallel flat fading subchannels. The conventional and iterative reconstruction of transmitted data in step k, after removing CP are described as follows. In conventional OFDM systems (see Fig. 2), the received signal after the FFT transform can be written as:

$$\begin{aligned} \mathbf{r^k_B} &= \mathbf{F}_N \mathbf{H_{AB}} \mathbf{s^k_A} + \mathbf{F}_N \nu_{\mathbf{AB}} = \mathbf{F}_N \mathbf{H_{AB}} \mathbf{F}_N^H \mathbf{G}_f \mathbf{c'^k_A} + \mathbf{F}_N \nu_{\mathbf{AB}} \\ &= \mathbf{D_{AB}} \mathbf{G}_f \mathbf{c'^k_A} + \mathbf{F}_N \nu_{\mathbf{AB}}, \end{aligned} \tag{2}$$

in which

$$\begin{aligned} \mathbf{D_{AB}} &= \mathrm{diag}(H_{AB}(0),\ H_{AB}(1),\ \ldots,\ H_{AB}(N-1)) \\ &= \mathbf{F}_N \mathbf{H_{AB}} \mathbf{F}_N^H, \end{aligned} \tag{3}$$

where

$$H_{AB}(n) = \sum_{l=0}^{L_{AB}} h_{AB}(l) \exp(-j2\pi n 1/N), \tag{4}$$

is the frequency response of the underlying finite impulse response (FIR) channel evaluated at the FFT grid, and $\nu_{\mathbf{AB}}$ denotes the white Gaussian noise with zero mean and variance N_0. Hence, after frequency domain equalization (FDE) block, we obtain $\hat{\mathbf{s}}_{\mathbf{A}}^{\mathbf{k}} = \mathbf{G}_f \mathbf{c}_{\mathbf{A}}^{\prime\mathbf{k}} + \mathbf{D}_{\mathbf{AB}}{}^{-1}\mathbf{F}_N \nu_{\mathbf{AB}}$. The statement of the problem is that given the output $\mathbf{G}_f \mathbf{c}_{\mathbf{A}}^{\prime\mathbf{k}}$ vector, we wish to find the input vector $\mathbf{c}_{\mathbf{A}}^{\prime\mathbf{k}}$, i.e., the inverse of the system. Many schemes have been proposed to recover the missing samples using the remaining samples of the signal. Some of these schemes use techniques such as compressive sensing [34], linear canonical transform [35], a series of filtering operations [36], [37], approximation methods [38] and some matrix-based projections [39]. A simple remedy for this problem is the application of zero-forcing (ZF) equalizer. As shown in the conventional receiver in Fig. 2, $\mathbf{G}_f^{\dagger}$ is cascaded at the end of node B's receiver to obtain node A's data, $\mathbf{c}_{\mathbf{A}}^{\prime\mathbf{k}}$, where † denotes Moore-Penrose pseudo-inverse. Unfortunately, the direct ZF method requires the inversion of an $N \times N$ matrix of $\mathbf{G}_f$. When N is large, the computational complexity can become prohibitively high. It has been noted that iterative procedures are suitable to manipulate large matrices as they are robust and less susceptible to numerical errors than direct methods [40]. We will show that the iterative receiver in Fig. 2 can calculate $\mathbf{G}_f^{\dagger}$ indirectly with the finite number of iterations. Thus, $\mathbf{c}_{\mathbf{A}}^{\prime\mathbf{k}}$ can be completely obtained from a part of transmitted data, $\mathbf{s}_{\mathbf{A}}^{\mathbf{k}}$, in node B. The computation complexity of the proposed receiver is shown in Appendix A.

B. Iterative Receiver

The first two stages of the iterative receiver in Fig. 2 are similar to the conventional receiver. Therefore,

$$\hat{\mathbf{s}}_{A}^{k} = \mathbf{G}_f \mathbf{c}_{\mathbf{A}}^{\prime\mathbf{k}} + \mathbf{D}_{\mathbf{AB}}{}^{-1}\mathbf{F}_N \nu_{\mathbf{AB}}. \tag{5}$$

Note that if we use the iterative interpolator before FFT processing in time domain at the receiver, we should devise a complicated computational receiver which removes both the frequency-selective and $\mathbf{G}_t$ effects. The iterative interpolator model is a nonlinear block, as it will be explained in the sequel. Thus, the multiplication of this nonlinear block by the circulant matrix of $\mathbf{H}_{\mathbf{AB}}$ would not be yet a circulant matrix. Hence, applying IFFT transform at the transmitter and taking FFT at the receiver cannot convert the time-domain overall channel into the diagonal matrix in the frequency domain. Therefore, a complicated time-domain equalizer whose implementation is not straightforward should be devised for this OFDM system. Henceforth, frequency domain interpolation (see Fig. 2) is considered in the proposed method. After FFT processing and FDE equalization stages, in uniform sampling block, node B sets the symbols on positions where punctured by the matrix of $\mathbf{G}_t$, to zero. To this end, the frequency domain signal of $\hat{\mathbf{s}}_{\mathbf{A}}^{\mathbf{k}}$ is transformed into the time domain by taking $N-$point IFFT. Afterwards, $\mathbf{F}_N^H \hat{\mathbf{s}}_{\mathbf{A}}^{\mathbf{k}}$ is multiplied by the time domain puncturing matrix of $\mathbf{G}_t$ in time domain. The overall processing of the uniform sampling stage can be concisely written as $\mathbf{G}_t \mathbf{F}_N^H$. Note that at the output of this stage, node B has the uniform sampled version of node A's data because of the puncturing matrix $\mathbf{G}_t$, since it discards some symbols from each OFDM symbol in time domain. To reconstruct the lost symbols from the remaining ones, $\Psi_{\mathbf{A}} = \mathbf{G}_t \mathbf{F}_N^H \hat{\mathbf{s}}_{\mathbf{A}}^{\mathbf{k}}$, we can use the iterative reconstruction block shown in Fig. 2 which uses the puncturing matrix $\mathbf{G}_t$. This nonlinear iterative reconstruction block is a modified version of the Marvasti method [41] and it can be modelled as:

$$\begin{cases} \widetilde{\mathbf{s}}_{\mathbf{A}}^{ik} = \Psi_{\mathbf{A}} + (\mathbf{I}_N - \mathbf{G}_t)\, \widetilde{\mathbf{s}}_{\mathbf{A}}^{(i-1)k} & i > 0 \\ \widetilde{\mathbf{s}}_{\mathbf{A}}^{0k} = \Psi_{\mathbf{A}} & i = 0, \end{cases} \tag{6}$$

where $\widetilde{\mathbf{s}}_{\mathbf{A}}^{ik}$ and $\widetilde{\mathbf{s}}_{\mathbf{A}}^{(i-1)k}$ are the reconstructed vector of node A's data in i^{th} and $(i-1)^{\text{th}}$ iteration for k^{th} step of cooperation, respectively. It is shown in Appendix B that the iterative method is convergent. Hence, asymptotically $\widetilde{\mathbf{s}}_{\mathbf{A}}^{ik} = \widetilde{\mathbf{s}}_{\mathbf{A}}^{(i-1)k}$. Therefore from equation (6), one can easily find the steady state value of $\widetilde{\mathbf{s}}_{\mathbf{A}}^{\infty k} = \mathbf{G}_t^{\dagger} \widetilde{\mathbf{s}}_{\mathbf{A}}^{0k} = \mathbf{F}_N^H \mathbf{G}_f^{\dagger} \mathbf{F}_N \widetilde{\mathbf{s}}_{\mathbf{A}}^{0k}$ for the iterative method. It holds that:

$$\begin{aligned} \widetilde{\mathbf{s}}_{\mathbf{A}}^{0k} &= \Psi_{\mathbf{A}} = \mathbf{G}_t \mathbf{F}_N^H \hat{\mathbf{s}}_{\mathbf{A}}^{\mathbf{k}} = \mathbf{F}_N^H \mathbf{G}_f \mathbf{F}_N \mathbf{F}_N^H \hat{\mathbf{s}}_{\mathbf{A}}^{\mathbf{k}} \\ &= \mathbf{F}_N^H \mathbf{G}_f \left(\mathbf{G}_f \mathbf{c}_{\mathbf{A}}^{\prime\mathbf{k}} + \mathbf{D}_{\mathbf{AB}}{}^{-1}\mathbf{F}_N \nu_{\mathbf{AB}} \right) \\ &= \mathbf{F}_N^H \mathbf{G}_f \mathbf{c}_{\mathbf{A}}^{\prime\mathbf{k}} + \mathbf{F}_N^H \mathbf{G}_f \mathbf{D}_{\mathbf{AB}}^{-\mathbf{1}} \mathbf{F}_N \nu_{\mathbf{AB}}, \end{aligned} \tag{7}$$

where the last equation is obtained from the fact that $(\mathbf{G}_f)^q = \mathbf{F}_N^H (\mathbf{G}_t)^q \mathbf{F}_N = \mathbf{F}_N^H \mathbf{G}_t \mathbf{F}_N = \mathbf{G}_f$ for $q = 1, 2, \ \ldots$ because $\mathbf{G}_t$ is diagonal with diagonal entries given by $g_{tm} \in \{0, 1\}$. Thus, we can substitute (7) into $\widetilde{\mathbf{s}}_{\mathbf{A}}^{\infty k} = \mathbf{F}_N^H \mathbf{G}_f^{\dagger} \mathbf{F}_N \widetilde{\mathbf{s}}_{\mathbf{A}}^{0k}$ and obtain $\widetilde{\mathbf{s}}_{\mathbf{A}}^{\infty k} = \mathbf{F}_N^H \mathbf{c}_{\mathbf{A}}^{\prime\mathbf{k}} + \mathbf{F}_N^H \mathbf{D}_{\mathbf{AB}}{}^{-1}\mathbf{F}_N \nu_{\mathbf{AB}}$. By taking $N-$point FFT at the ending block of the iterative receiver Fig. 2, node B can completely estimate $\hat{\mathbf{c}}_{\mathbf{A}}^{\prime\mathbf{k}}$ at the infinite iteration as follows

$$\hat{\mathbf{c}}_{\mathbf{A}}^{\prime\mathbf{k}} = \mathbf{c}_{\mathbf{A}}^{\prime\mathbf{k}} + \mathbf{D}_{\mathbf{AB}}{}^{-1}\mathbf{F}_N \nu_{\mathbf{AB}}. \tag{8}$$

Proposition 1: It can also be shown that $\hat{\mathbf{c}}_{\mathbf{A}}^{\prime\mathbf{k}}$ for an arbitrary i^{th} iteration can be obtained from

$$\hat{\mathbf{c}}_{\mathbf{A}}^{\prime\mathbf{k}} = \mathbf{F}_N \left(\mathbf{I}_N - (\mathbf{I}_N - \mathbf{G}_t)^{i+1} \right) (\mathbf{G}_t \mathbf{F}_N^H \mathbf{c}_{\mathbf{A}}^{\prime\mathbf{k}} + \mathbf{F}_N^H \mathbf{D}_{\mathbf{AB}}{}^{-1}\mathbf{F}_N \nu_{\boldsymbol{AB}}). \tag{9}$$

Proof: See Appendix C. □

Therefore, it is shown from (8) that the iterative method indirectly reconstructs the missing samples at the infinity of iteration $i \to \infty$. Also, the reconstructed OFDM symbol in equation (9) is obtained, for any arbitrary iteration i.

C. Oversampled OFDM System and Convergent Iterative Receiver

Although we have analytically proved that the iterative reconstruction block at node B can remove the effects of puncturing matrix $\mathbf{G}_t$ for infinite iteration, the proposed iterative method does not converge due to the Nyquist theorem. If we denote P_ε as the symbol probability of loss, then it has been shown that the complement of $1 - P_\varepsilon$ is the sampling rate normalized by the Nyquist rate, needed for error-free transmission [42]. If we define n_0 as the number of zero entries on the $N \times N$ diagonal puncturing matrix $\mathbf{G}_t$, the probability of loss at the input of receiver node B would be $P_\varepsilon = n_0/N$. Hence, for error-free transmission, the normalized sampling rate by the Nyquist rate of $N/(N-n_0)$ should be selected at the transmit side. It is obvious that by inserting $(\frac{N}{N-n_0}-1)K$ zeros at the end of initial block $\mathbf{c_A^k}$ before applying $N-$point IFFT at the transmit side, the oversampling factor $N/(N-n_0)$ can be obtained from

$$\mathbf{c_A'^k} = \Bigg[\underbrace{\overbrace{c_A'^k(1), c_A'^k(2), \ldots, c_A'^k(K)}^{K},\ \underbrace{0, \ldots, 0}_{\left(\frac{N}{N-n_0}-1\right)K}}_{N \text{ elements}}\Bigg]^T. \quad (10)$$

Note that $\mathbf{c_A'^k}$ in the FFT domain can act as an (N, K) code which is a special case of Reed-Solomon codes in real field, as opposed to finite Galois field, which under certain conditions is capable of correcting $N-K = (\frac{N}{N-n_0}-1)K$ erasures [42].

For example, consider $N = 4$ and $\mathbf{G}_t = \begin{pmatrix} 1&0&0&0\\0&0&0&0\\0&0&1&0\\0&0&0&0 \end{pmatrix}$, in which the number of diagonal entries equal to zero is 2; thus $n_0 = 2$ and

$$\hat{\mathbf{s}}_\mathbf{A}^\mathbf{k} = \begin{pmatrix} s_{1A}^k \\ 0 \\ s_{3A}^k \\ 0 \end{pmatrix}. \quad (11)$$

It shows that the first and third samples of node A's data are transmitted in cooperation step k, and the second and fourth samples are dropped. Hence, the probability of loss would be $P_\varepsilon = 0.5$, and the minimum sampling rate normalized by the Nyquist rate, needed for error-free transmission, is $\frac{1}{1-P_\varepsilon} = 2$. The receive side for oversampled OFDM system which uses the convergent iterative reconstruction block is also depicted in Fig. 2. Note that for reversing the operations implemented at the transmitter, after frequency domain channel equalization at the receiver, we first set the time domain punctured samples in $\hat{\mathbf{s}}_\mathbf{A}^\mathbf{k}$ to zeros, by the uniform sampling block, $\Psi_\mathbf{A} = \mathbf{G}_t\mathbf{F}_N^H\hat{\mathbf{s}}_\mathbf{A}^\mathbf{k}$, and then we set frequency domain erasures, $(\frac{N}{N-n_0}-1)K$ tail end samples of $\Psi_\mathbf{A}$, to zeros, by LPF block. To erase frequency domain erasures from the time domain signal of $\Psi_\mathbf{A}$ in LPF block, we first take an $N-$point FFT to transform $\Psi_\mathbf{A}$ into frequency domain, $\mathbf{F}_N\Psi_\mathbf{A}$, and then erase frequency domain erasures through the erasure matrix of $\mathbf{E} = \mathrm{diag}([\mathbf{I}_K\, \mathbf{0}_{N-K}])$, and an $N-$point IFFT brings back the signal to time domain, $\widetilde{\Psi}_\mathbf{A} = \mathbf{F}_N^H\mathbf{E}\mathbf{F}_N\Psi_\mathbf{A}$ which should feed into the iterative reconstruction block. By substituting $\mathbf{F}_N^H\mathbf{E}\mathbf{F}_N\mathbf{G}_t$, and $\mathbf{F}_N^H\mathbf{E}\mathbf{F}_N\Psi_\mathbf{A}$ for $\mathbf{G}_t$, and $\Psi_\mathbf{A}$ in equation (6), then following the steps to obtain (6)-(8) we can write

$$\hat{\mathbf{c}}_\mathbf{A}'^\mathbf{k} = \mathbf{F}_N \times \left(\mathbf{I}_N - (\mathbf{I}_N - \mathbf{F}_N^H\mathbf{E}\mathbf{F}_N\mathbf{G}_t)^{i+1}\right) \times (\mathbf{G}_t\mathbf{F}_N^H\mathbf{c_A'^k} + \mathbf{F}_N^H\mathbf{D_{AB}^{-1}}\mathbf{F}_N\nu_\mathbf{AB})\mathbf{D_{AB}}^{-1}. \quad (12)$$

Also, in Appendix D, we prove that for infinite iteration we have:

$$\hat{\mathbf{c}}_\mathbf{A}'^\mathbf{k} = \mathbf{c_A'^k} + \mathbf{D_{AB}^{-1}}\mathbf{F}_N\nu_\mathbf{AB}, \mathbf{D_{AB}}^{-1} \quad (13)$$

which shows that node B can completely recover node A's data from its fraction transmitted in cooperation step k. The whole cooperative process is separated into two consecutive symbol periods. Hence, the received signals after $N-$point FFT processing at destination node D in cooperation steps k and $k+1$ can be summarized as follows:

$$\begin{aligned} &\text{step } k: \ \mathbf{r_D}^\mathbf{k} = \mathbf{D_{AD}}\mathbf{G}_f\mathbf{c_A'^k} + \mathbf{F}_N\nu_\mathbf{AD} \\ &\text{step } k+1: \ \mathbf{r_D}^\mathbf{k+1} = \mathbf{D_{BD}}\left(\mathbf{I}_N - \mathbf{G}_f\right)\hat{\mathbf{c}}_\mathbf{A}'^\mathbf{k} + \mathbf{F}_N\nu_\mathbf{BD}, \end{aligned} \quad (14)$$

in which, node A transmits a fraction of its own data, $\mathbf{G}_f\mathbf{c_A'^k}$, in cooperation step k, and node B transmits the remaining data of node A, $\left(\mathbf{I}_N - \mathbf{G}_f\right)\hat{\mathbf{c}}_\mathbf{A}'^\mathbf{k}$, in cooperation step $k+1$. By substituting (12) into (14) we have:

$$\text{step } k+1: \ \mathbf{r_D}^\mathbf{k+1} = \mathbf{D_{BD}}\left(\mathbf{I}_N - \mathbf{G}_f\right)\mathbf{F}_N \times \left(\mathbf{I}_N - (\mathbf{I}_N - \mathbf{F}_N^H\mathbf{E}\mathbf{F}_N\mathbf{G}_t)^{i+1}\right)\mathbf{G}_t\mathbf{F}_N^H\mathbf{c_A'^k} + \mathbf{n_{BD}}, \quad (15)$$

where

$$\mathbf{n_{BD}} = \mathbf{D_{BD}}\left(\mathbf{I}_N - \mathbf{G}_f\right)\mathbf{F}_N \times \left(\mathbf{I}_N - (\mathbf{I}_N - \mathbf{F}_N^H\mathbf{E}\mathbf{F}_N\mathbf{G}_t)^{i+1}\right)\mathbf{F}_N^H\mathbf{D_{AB}}^{-1}\mathbf{F}_N\nu_\mathbf{AB} + \mathbf{F}_N\nu_\mathbf{BD}, \quad (16)$$

is noise at the destination node D. The following operation is performed on $\mathbf{r_D}^\mathbf{k+1}$ to unify the noise variance to N_0. (17), as shown at the bottom of this page.

The destination node D can employ maximum-ratio combining (MRC) of $\mathbf{r_D}^\mathbf{k}$ and $\overline{\mathbf{r}}_\mathbf{D}^\mathbf{k+1}$ to yield:

$$\mathbf{r_D} = \mathrm{diag}(\mathbf{w_1})\mathbf{r_D^k} + \mathrm{diag}(\mathbf{w_2})\overline{\mathbf{r}}_\mathbf{D}^\mathbf{k+1}, \quad (18)$$

where $\mathbf{w_1}$ and $\mathbf{w_2}$ denote MRC coefficients. MRC is employed at the destination to maximize the received signal-to-noise ratio (SNR). Then, the single-tap equalizers, e.g., ZF or minimum mean-square error (MMSE), can be applied for the channel equalization whereas they do not change the SNR of the received symbols. The symbol detection performance is related to the effective SNR of the m^{th} subchannel, denoted

$$\overline{\mathbf{r}}_\mathbf{D}^\mathbf{k+1} = \underbrace{\left(\left|\mathbf{D_{BD}}\left(\mathbf{I}_N - \mathbf{G}_f\right)\mathbf{F}_N\left(\mathbf{I}_N - (\mathbf{I}_N - \mathbf{F}_N^H\mathbf{E}\mathbf{F}_N\mathbf{G}_t)^{i+1}\right)\mathbf{F}_N^H\mathbf{D_{AB}}^{-1}\mathbf{F}_N\right|^2 + \mathbf{F}_N\right)^{\frac{-1}{2}}}_{\theta}\mathbf{r_D}^\mathbf{k+1}. \quad (17)$$

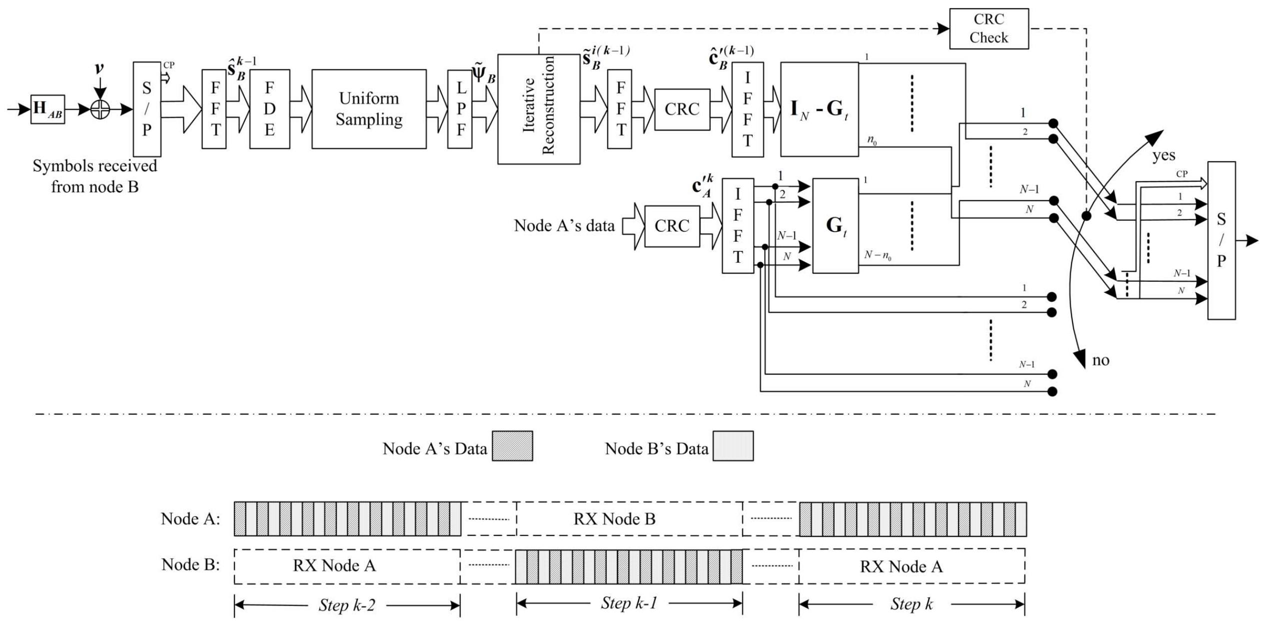

Fig. 3. Top: Node A in cooperation step k in proposed coded cooperative diversity based on superposition modulation for oversampled OFDM systems. Bottom: Coded cooperation based on superposition modulation implementation for a system using TDMA.

by $\beta(m)$ for MRC [43], i.e.,

$$\beta_D(m) = \beta_D^{\mathbf{k}}(m) + \beta_D^{\mathbf{k+1}}(m). \tag{19}$$

Note that nodes A and B in the proposed cooperative transmission can be modelled as the precoded OFDM systems with the precoder of $\mathbf{G}_f$ in cooperation step k and the precoder of $\mathbf{\Omega} = (\mathbf{I}_N - \mathbf{G_f})\,\mathbf{F}_N\left(\mathbf{I}_N - (\mathbf{I}_N - \mathbf{F}_N^H\mathbf{E}\mathbf{F}_N\mathbf{G}_t)^{i+1}\right)\mathbf{G}_t\mathbf{F}_N^H$ in cooperation step $k{+}1$ respectively, (see equations (14) and (15)). Thus, following the approach in [33], we can compute the SNR of the mth subchannel for the received precoded OFDM signal in cooperation step k as:

$$\beta_D^{\mathbf{k}}(m) = \frac{\gamma_1}{\sum_{k=0}^{N-1} \frac{\left|\mathbf{G}_{f(k,m)}\right|^2}{\left|\mathbf{D}_{AD(k,k)}\right|^2}}, \tag{20}$$

for $m = 0, 1, \ldots, N-1$ and $\mathbf{G}_f$ as the precoder. For the precoded OFDM with $\mathbf{\Omega}$ as the precoder for the received signal in cooperation step $k+1$, we have

$$\beta_D^{\mathbf{k+1}}(m) = \frac{\gamma_2}{\sum_{k=0}^{N-1} \frac{\left|\left((\mathbf{I}_N - \mathbf{G}_f)\mathbf{F}_N\left(\mathbf{I}_N - (\mathbf{I}_N - \mathbf{F}_N^H\mathbf{E}\mathbf{F}_N\mathbf{G}_t)^{i+1}\right)\mathbf{G}_t\mathbf{F}_N^H\right)_{(k,m)}\right|^2}{\left|\theta D_{BD_{(k,k)}}\right|^2}}. \tag{21}$$

Note that $\gamma = \gamma_1 = \gamma_2 = \frac{\xi_{\mathbf{c}'^{\mathbf{k}}_{\mathbf{A}}}}{N_0}$ denotes the ratio of the transmitted symbol energy of $\mathbf{c}'^{\mathbf{k}}_{\mathbf{A}}$, compared to the noise variance at nodes B and D, respectively. For M-ary QAM modulation schemes, the symbol-error-rate (SER) (denoted by P) for the mth element of $\mathbf{r_D}$ is tightly upper-bounded by [43]:

$$P(m) = 4Q\left(\sqrt{\frac{3\beta_D(m)}{M-1}}\right), \tag{22}$$

where $Q(.)$ is the Gaussian Q-function.

III. Coded Cooperative Diversity Based on Superposition Modulation for Oversampled OFDM Signals

Although oversampling makes the iterative reconstruction block to converge, it decreases the bandwidth efficiency of transmission link. If node A transmits the estimated node B's data, transmitted in cooperation step $k-1$, on subcarriers filled by n_0 zero samples due to the puncturing matrix of $\mathbf{G}_t$, a better use of bandwidth would be possible. This bandwidth efficient coded cooperative diversity scheme based on superposition modulation for oversampled OFDM system is depicted in Fig. 3, where node A in the k^{th} step of cooperation transmits a fraction of its own data corresponding to $N - n_0$ non zero diagonal entries of $\mathbf{G}_t$. Node A also sends the remaining of the OFDM symbol for node B through the puncturing block of $\mathbf{I}_N - \mathbf{G}_t$ in cooperation step k, if it can successfully (as indicated by cyclic redundancy check (CRC) bits) recover the whole of B's data from the received segment by the iterative reconstruction method in cooperation step $k-1$. Coded cooperation based on superposition modulation implementation for a system using time division multiple access (TDMA) is depicted in Fig. 3. The key idea is that when A, for example in step k, acts as a relay for B, it simultaneously transmits a fraction of its own packet data, $\mathbf{c}'^{\mathbf{k}}_{\mathbf{A}}$, and the segment of packet for which it acts as relay, $\hat{\mathbf{c}}'^{\mathbf{k}-1}_{\mathbf{B}}$. If A in the cooperation step $(k-1)$ cannot detect node B's data, by checking CRC bits in the iterative reconstruction block, it just transmits its own data in cooperation step k. In cooperation step $k+1$, node B acts as relay for A and transmits its own data corresponding to $N - n_0$ non zero diagonal entries of $\mathbf{G}_t$ and the remaining of the OFDM symbol for node A through the puncturing block of $\mathbf{I}_N - \mathbf{G}_t$, if B could successfully recover the whole of A's data from the received segment by the iterative reconstruction method in cooperation step k. For successful reconstruction in both nodes, the received signals after $N-$point FFT processing at the destination node D in cooperation steps k and $k+1$ can be summarized as follows:

$$\begin{aligned} \text{step } k: \ \mathbf{r_D}^{\mathbf{k}} &= \mathbf{D_{AD}}\left(\mathbf{G}_f \mathbf{c'}^{\mathbf{k}}_{\mathbf{A}} + \left(\mathbf{I}_N - \mathbf{G}_f\right)\hat{\mathbf{c}}'^{\mathbf{k}-1}_{\mathbf{B}}\right) + \mathbf{F}_N \nu_{\mathbf{AD}} \\ \text{step } k+1: \mathbf{r_D}^{\mathbf{k+1}} &= \mathbf{D_{BD}}\left(\mathbf{G}_f \mathbf{c}'^{\mathbf{k+1}}_{\mathbf{B}} + \left(\mathbf{I}_N - \mathbf{G}_f\right)\hat{\mathbf{c}}'^{\mathbf{k}}_{\mathbf{A}}\right) \\ &\quad + \mathbf{F}_N \nu_{\mathbf{BD}}, \end{aligned} \tag{23}$$

in which, node A transmits a fraction of its own data, $\mathbf{G_f c'^k_A}$, and a fraction of estimated node B's data, $\left(\mathbf{I}_N - \mathbf{G}_f\right)\hat{\mathbf{c}}'^{\mathbf{k}-1}_{\mathbf{B}}$, in cooperation step k, and node B transmits the remaining data of node A, $\left(\mathbf{I}_N - \mathbf{G}_f\right)\hat{\mathbf{c}}'^{\mathbf{k}}_{\mathbf{A}}$, and its own data, $\mathbf{G}_f \mathbf{c}'^{\mathbf{k+1}}_{\mathbf{B}}$, in cooperation step $k+1$.

A. *Cooperation Level and Sampling Rate*

The cooperation level is defined as the percentage of each OFDM symbol that the relay node transmits for its user node. In the proposed coded cooperative diversity scheme based on superposition modulation, each node transmits for its partner only on positions corresponding to n_0, i.e., zero diagonal entries of the puncturing matrix $\mathbf{G}_t$ (see Fig. 3). Hence, the cooperation level is $\frac{n_0}{N}$, which is similar to the probability of loss of P_ε as defined in Section II. Thus, different levels of cooperation are simply provided by changing n_0 as long as the Nyquist theorem is guaranteed, for reconstructing the lost samples. Thus, for error-free transmission with the cooperation level of $\frac{n_0}{N}$, the minimum normalized sampling rate by the Nyquist rate of $N/(N-n_0)$ is required. For example, consider $N = 4$ and $\mathbf{G}_t = \begin{pmatrix} 1 & 0 & 0 & 0 \\ 0 & 0 & 0 & 0 \\ 0 & 0 & 1 & 0 \\ 0 & 0 & 0 & 0 \end{pmatrix}$, where $n_0 = 2$ and $P_\varepsilon = 1/2$. If node A transmits a fraction of node B's data transmitted in cooperation step $k-1$ on zero entries on the diagonal matrix $\mathbf{G}_t$ positions, i.e.

$$\hat{\mathbf{s}}^{\mathbf{k}}_{\mathbf{A}} = \begin{pmatrix} s^k_{1A} \\ s^{k-1}_{2B} \\ s^k_{3A} \\ s^{k-1}_{4B} \end{pmatrix}, \tag{24}$$

then a cooperation level 50% ($n_0/N \times 100\%$) is obtained, while $N/(N-n_0) = 2$ is the minimum sampling rate normalized by the Nyquist rate, required for error-free transmission.

IV. Results and Discussion

In this section, we present Monte-Carlo simulation results for oversampled OFDM coded cooperative systems which have been described and analyzed in this paper over frequency-selective Rayleigh fading channels. Unless otherwise is specified, the system parameters assumed in the simulation are: $K = 32$, length of data block with Gray-mapped 16QAM modulation on each entry; $N/(N-n_0) = 4$ the oversampling factor as in [30] for PAPR reduction considerations; $N = 128$ number of subcarriers; and $i = 10$ number of iterations

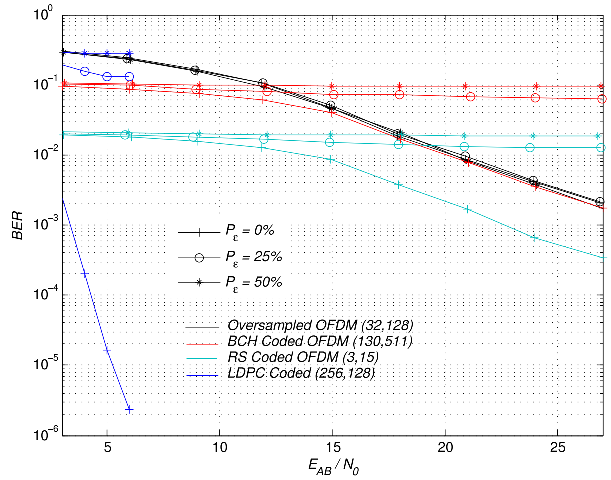

Fig. 4. BER performance of the oversampled OFDM, the (511, 130) BCH coded OFDM, the (15, 3) RS coded OFDM, and (256, 128) LDPC coded system versus E_{AB}/N_0 at the partner node B for different amount of information transmitted by node A in cooperation step k.

employed at the iterative receiver. First, we consider the cooperation step k in which node A transmits just a fraction of its data towards node B through the A $\to$ B faded link. Under this scenario, Fig. 4 compares the bit error rate (BER) performance of the oversampled OFDM system with that of the (511, 130) BCH coded OFDM system, the (15, 3) Reed Solomon (RS) coded OFDM system, and (256, 128) LDPC coded system. As we analytically proved in (12) and (8), the convergent iterative receiver at node B can perfectly reconstruct $\mathbf{c}'^{\mathbf{k}}_{\mathbf{A}}$ from a part of transmitted oversampled OFDM data, $\mathbf{s}^{\mathbf{k}}_{\mathbf{A}}$. Note that as we discussed in Section II. C, perfect recovery and error-free transmission is guaranteed if sufficient redundancy is provided. Hence, with an oversampling factor of $N/(N-n_0) = 4$ at node A and probability of loss of $P_\varepsilon = n_0/N = 25\%$ or 50% as considered in Fig. 4, perfect recovery is ensured. Note that the BER performance for any value of probability of loss is comparable with the condition in which 100% data is available at node B, only with $i = 10$ iterations. This shows that the proposed iterative receiver at node B has a converging behaviour as proved in Appendix B. In low SNR regime, random noise effects are more harmful, so we have low-quality samples in $\mathbf{s}^{\mathbf{k}}_{\mathbf{A}}$. To overcome the random noise, iterative reconstruction of $\mathbf{c}'^{\mathbf{k}}_{\mathbf{A}}$ from these low-quality samples in $\mathbf{s}^{\mathbf{k}}_{\mathbf{A}}$ would not be useful in compare to the other channel coded OFDM systems. Clearly, using the oversampled OFDM system to completely recover the $\mathbf{c}'^{\mathbf{k}}_{\mathbf{A}}$, with the other channel coding techniques, e.g. LDPC code, to overcome channel random noise will significantly improve the performance at the expense of more bandwidth, and complexity in low SNR regime. Fig. 5 shows the BER performance of the coded cooperative diversity scheme for oversampled OFDM system, the BCH coded cooperation, and the RS coded cooperative diversity. We assume that node A transmits just a fraction of its own data towards the destination node D through the A $\to$ D faded link in cooperation step k, and node B transmits the remaining part of node A's data through the B $\to$ D faded link in cooperation step $k+1$. Node D's estimates are

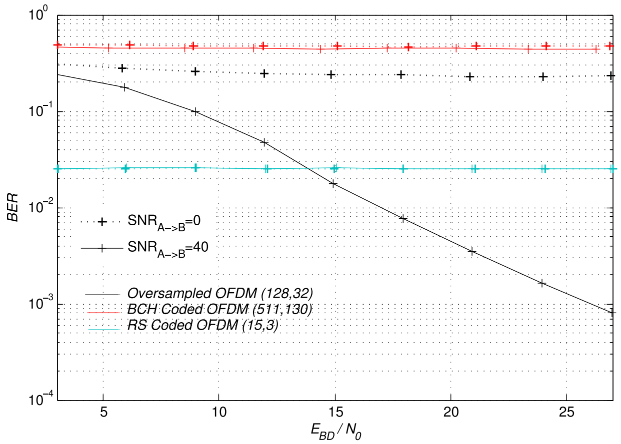

Fig. 5. Node A's BER versus the B → D uplink channel's E_{BD}/N_0 for the coded cooperative diversity in the oversampled OFDM system, the (511, 130) BCH coded OFDM system, and the (15, 3) RS coded OFDM system.

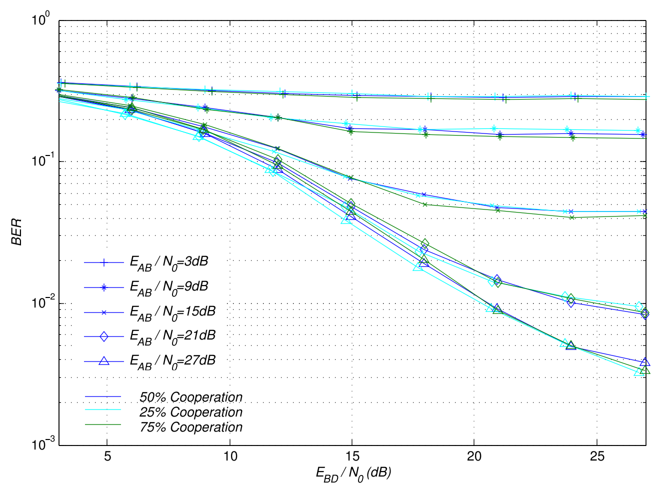

Fig. 6. Node A's BER versus the B → D uplink channel's E_{BD}/N_0 for the coded cooperative diversity in the oversampled OFDM system for different values of E_{AB}/N_0 and different cooperation levels. The destination node D only uses the received signal in cooperation step $k+1$ for node A's signal estimation.

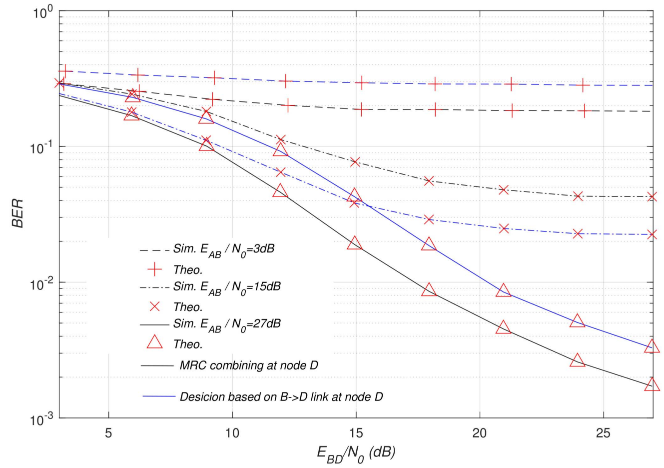

Fig. 7. Node A's BER versus the B → D uplink channel's E_{BD}/N_0 for the coded cooperative diversity in the oversampled OFDM system for different values of E_{AB}/N_0 and different cooperation levels for two detection rules at the destination node D. The destination node D only uses the received signal in cooperation step $k+1$ or uses MRC combination of the received signals in cooperation steps of k and $k+1$ for node A's signal estimation.

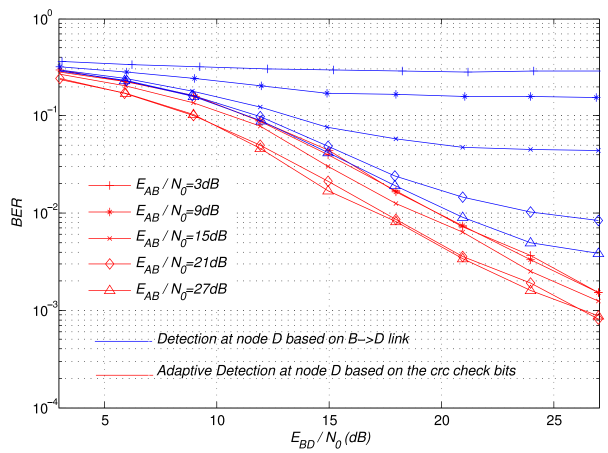

Fig. 8. Node A's BER versus the B → D uplink channel's E_{BD}/N_0 for the coded cooperative diversity based on superposition modulation using the adaptive detection manner and the coded cooperative diversity for the oversampled OFDM system using the simple detection at node D.

based only on the received signal in cooperation step $k+1$ in Fig. 5. $SNR_{AB} = 0$dB and $SNR_{AB} = 40$dB have been considered in Fig. 5 with dotted and solid lines, respectively. Although the cooperation level of 50% is only depicted with "+" marker in Fig. 5, it is obvious that in high/low levels of cooperation due to the weak reconstruction ability at node B (see Fig. 4), (511, 130) BCH/(15, 3) RS coded cooperative systems cannot utilize cooperation benefits, even in conditions that the inter-user channel has a good quality, i.e. $SNR_{AB} = 40$dB. In low / high levels of cooperation, node B / A transmits a small fraction of node A's / its own data in cooperation step $k+1$ / k and hence node D / B cannot reconstruct all of node A's data from its small fraction. Hence, the coded cooperation degrades the BER performance of the conventional (511, 130) BCH/(15, 3) RS coded cooperative systems due to their weak ability in reconstructing lost samples. Fig. 6 shows the BER performance of the coded cooperative diversity for oversampled OFDM systems for different values of E_{AB}/N_0 and different cooperation levels. For higher values of E_{AB}/N_0, BER performance is improved due to the more reliable signal at node D. Note that BER performance for 25%, 50%, and 75% cooperation levels is the same because the iterative reconstruction algorithm at node D can perfectly estimate $\mathbf{c}'^{\mathbf{k}}_{\mathbf{A}}$ from a fraction that is estimated and then transmitted by node B. Fig. 7 shows the BER performance of the coded cooperative diversity scheme for oversampled OFDM systems for different values of E_{AB}/N_0 for two different detection methods at the destination node D. In the first method, detection is performed at the receiver based on the received signal from node B in cooperation step $k+1$. In the second method, node D uses MRC combining of the received signals from both of the A and B nodes in cooperation steps k and $k+1$. We note that in both cases shown in Fig. 7, simulation results match the analytical results obtained from (14)-(22), where BER is approximately obtained from SER in (22) as $P_{BER}(m) \approx P(m)/\log_2^M$ [43]. Fig. 8 compares the BER performance of the coded cooperative diversity scheme based on superposition modulation for oversampled OFDM systems using the adaptive detector at the destination terminal D with that of the coded cooperative diversity scheme for oversampled OFDM systems employing the simple detector at the destination terminal D for different inter-user channel qualities (E_{AB}/N_0). The simple detector estimates $\mathbf{c}'^{\mathbf{k}}_{\mathbf{A}}$ based on the received signal at node D in cooperation step $k+1$. In the adaptive detector, a 16-bit CRC code is employed with a generator polynomial given by the coefficients 15935 (hexadecimal notation). If node B can recover node A's data, transmitted in cooperation step k, as indicated by the CRC bits, MRC combining of the received signals from both cooperation steps k and $k+1$ is considered in the adaptive receiver at node D. Finally, if the partner terminal B cannot recover node A's OFDM symbol successfully, just the transmitted signal in cooperation step k is applied for node A's data recovery at node D.

V. Conclusions

We proposed a coded cooperative diversity scheme for uncoded OFDM signals based on the oversampling potential in OFDM systems instead of using extra channel coding schemes at the cooperative nodes. We analytically proved that instead of using the complicated channel decoding algorithms, a simple iterative detector using the uniform sampling block can be utilized for perfect recovery of the user's entire data from its transmitted partitioned version at the partner and the destination nodes. We also showed that different cooperation levels are easily obtained by changing the value of the oversampling factor $N/(N-n_0)$, defined as the size of zero samples sequence padded before the IFFT processing at the transmitting side of the cooperative nodes. For bandwidth efficiency, in subcarriers where the cooperative nodes transmit zero samples in each OFDM frame, we proposed coded cooperative diversity based on superposition modulation in which each user node uses the known subcarriers of zero samples in each OFDM frame for transmitting a fraction of its partner node's data. Simulation results reveal significant BER improvements of the proposed method over the conventional coded cooperative ones. The extension of proposed model to multiple relays [44] is straightforward. However, the mathematical analysis for dividing data packets of different users, relay selection issues, and the trade-off between minimum oversampling needed for errorless transmission, and the cooperation level will be derived in our future work.

Appendix A
Computational Complexity

We discuss here the computational complexity of the proposed iterative receiver in (34). Note that $\mathbf{G}_t = \operatorname{diag}(g_{t1},\ldots,g_{tN})$, $g_{tm}\in\{0,1\}$, $\mathbf{F}_N^H$ is Hermitian transpose of a $N\times N$ DFT matrix with $\left[\mathbf{F}_N\right]_{n,k} = N^{-(\frac{1}{2})}\exp\left(-j2\pi nk/N\right)$, $\hat{\mathbf{s}}^{\mathbf{k}}_{\mathbf{A}}$ is the $N\times 1$ input vector of the nonuniform sampling block, and $\mathbf{E}=\operatorname{diag}([\mathbf{I}_K\mathbf{0}_{N-K}])$ is the $N\times N$ erasure matrix. For the proposed iterative receiver, the calculation of $\mathbf{F}_N^H\hat{\mathbf{s}}^{\mathbf{k}}_{\mathbf{A}}$ requires $2N\log_2^N$ multiplications and $3N\log_2^N$ additions. Also, multiplication of $\mathbf{G}_t$ by $\mathbf{F}_N^H\hat{\mathbf{s}}^{\mathbf{k}}_{\mathbf{A}}$ requires N real multiplications. Thus, in order to produce the signal $\Psi_{\mathbf{A}}$, $2N\log_2^N+N$ multiplications are needed. In order to find $\tilde{\Psi_{\mathbf{A}}}$, we need $6N\log_2^N+N$ multiplications and $9N\log_2^N$ additions. This is due to the fact that calculation of $\mathbf{F}_N\Psi_{\mathbf{A}}$ requires $4N\log_2^N+N$ multiplications and $6N\log_2^N$ additions. Note that in $\mathbf{E}\mathbf{F}_N\Psi_{\mathbf{A}}$ the simple substitution is performed. Thus, the computational complexity of $\mathbf{E}\mathbf{F}_N\Psi_{\mathbf{A}}$ and $\mathbf{F}_N\Psi_{\mathbf{A}}$ are the same. To compute $\mathbf{F}_N^H\mathbf{E}\mathbf{F}_N\Psi_{\mathbf{A}}$, another $2N\log_2^N$ multiplications and $3N\log_2^N$ additions are needed.

Also, for each step i of the iterative receiver in (34) in the worst case, N additions for $\mathbf{I}_N-\tilde{\mathbf{G}}_t$, N^2 multiplications and $N(N-1)$ additions for $\left(\mathbf{I}_N-\tilde{\mathbf{G}}_t\right)\tilde{\mathbf{s}}_A^{(i-1)k}$, and N^2 additions for $\tilde{\Psi_{\mathbf{A}}}+\left(\mathbf{I}_N-\tilde{\mathbf{G}}_t\right)\tilde{\mathbf{s}}_A^{(i-1)k}$ are required. Therefore, the total number of multiplications and additions required by the proposed iterative receiver is $(6N\log_2^N+N+N^2)\times i$ and $(9N\log_2^N+2N^2)\times i$, respectively.

Simulation results show that our proposed iterative receiver is a fast iterative recovery technique that converges for $i=10$ number of iterations. Thus, the total number of multiplications and additions required by the proposed iterative receiver is $60N\log_2^N+10N+10N^2$ and $90N\log_2^N+20N^2$, respectively.

Appendix B
Convergence Conditions for the Iterative Method Defined in Equation (6)

We define the error vector as $\tilde{\mathbf{e}}^{ik}_{\mathbf{A}}=\tilde{\mathbf{s}}^{ik}_{\mathbf{A}}-\mathbf{F}_N^H\hat{\mathbf{s}}^k_{\mathbf{A}}$. By subtracting each side of equation (6) from $\mathbf{F}_N^H\hat{\mathbf{s}}^k_{\mathbf{A}}$ we find that the error at iteration i is

$$\begin{aligned}\tilde{\mathbf{s}}^{ik}_{\mathbf{A}}-\mathbf{F}_N^H\hat{\mathbf{s}}^k_{\mathbf{A}} &= \mathbf{G}_t\mathbf{F}_N^H\hat{\mathbf{s}}^{\mathbf{k}}_{\mathbf{A}}+(\mathbf{I}_N-\mathbf{G}_t)\,\tilde{s}^{(i-1)k}_{\mathbf{A}}-\mathbf{F}_N^H\hat{s}^k_A\\ &\Rightarrow \tilde{\mathbf{e}}^{ik}_{\mathbf{A}}=\tilde{\mathbf{e}}^{(i-1)k}_{\mathbf{A}}+\mathbf{G}_t\ (\mathbf{F}_N^H\hat{\mathbf{s}}^{\mathbf{k}}_{\mathbf{A}}-\tilde{\mathbf{s}}^{(i-1)k}_{\mathbf{A}})\\ &= \tilde{\mathbf{e}}^{(i-1)k}_{\mathbf{A}}-\mathbf{G}_t\tilde{\mathbf{e}}^{(i-1)k}_{\mathbf{A}}=(\mathbf{I}_N-\mathbf{G}_t)\,\tilde{\mathbf{e}}^{(i-1)k}_{\mathbf{A}}.\end{aligned}\tag{25}$$

Also, we have $\tilde{\mathbf{e}}^{0k}_{\mathbf{A}}=\tilde{\mathbf{s}}^{0k}_{\mathbf{A}}-\mathbf{F}_N^H\hat{\mathbf{s}}^k_{\mathbf{A}}=\Psi_{\mathbf{A}}-\mathbf{F}_N^H\hat{\mathbf{s}}^{\mathbf{k}}_{\mathbf{A}}$ for $i=0$. Thus, we can rewrite (6) as

$$\begin{cases}\tilde{\mathbf{e}}^{ik}_{\mathbf{A}}=(\mathbf{I}_N-\mathbf{G}_t)\,\tilde{\mathbf{e}}^{(i-1)k}_{\mathbf{A}} & i>0\\ \tilde{\mathbf{e}}^{0k}_{\mathbf{A}}=\Psi_{\mathbf{A}}-\mathbf{F}_N^H\hat{\mathbf{s}}^k_{\mathbf{A}} & i=0\end{cases}\tag{26}$$

$$\begin{aligned}&\overset{(17)}{\Rightarrow}\\ &\tilde{\mathbf{e}}^{ik}_{\mathbf{A}}=(\mathbf{I}_N-\mathbf{G}_t)^i\,\tilde{\mathbf{e}}^{0k}_{\mathbf{A}}=(\mathbf{I}_N-\mathbf{G}_t)^i\ (\Psi_{\mathbf{A}}-\mathbf{F}_N^H\hat{\mathbf{s}}^k_{\mathbf{A}})\\ &\quad=(\mathbf{I}_N-\mathbf{G}_t)^i\ (\mathbf{G}_t\mathbf{F}_N^H\hat{\mathbf{s}}^k_{\mathbf{A}}-\mathbf{F}_N^H\hat{\mathbf{s}}^k_{\mathbf{A}})\\ &\quad=-\,(\mathbf{I}_N-\mathbf{G}_t)^{i+1}\,\mathbf{F}_N^H\hat{\mathbf{s}}^k_{\mathbf{A}}.\end{aligned}\tag{27}$$

We are interested in the convergence of the sequence $\tilde{\mathbf{e}}^{ik}_{\mathbf{A}}$ when $i\to\infty$. Hence, we need to evaluate powers of $(\mathbf{I}_N-\mathbf{G}_t)^{i+1}$ as shown in (27). Assuming $\mathbf{G}_t$ is diagonal matrix $\mathbf{G}_t=\operatorname{diag}(g_{t1},\ldots,g_{tN})$, $g_{tm}\in\{0,1\}$ with eigenvalues $\lambda_1,\lambda_2,\cdots,\lambda_N$. Moreover, we have the following lemma.

Lemma 1: For every diagonalizable matrix $\mathbf{G}_t\in\Re^{n\times n}$, and $\|\mathbf{G}_t\|_p\le 1$, we conclude

$$(\mathbf{I}_N-\mathbf{G}_t)^{i+1}=\mathbf{V}\Lambda'^{i+1}\mathbf{V}^{-1},\tag{28}$$

where the columns of the matrix $\mathbf{V}$ are linearly independent eigenvectors of $\mathbf{G}_t$ and $\Lambda=diag(\lambda_1,\lambda_2,\cdots,\lambda_N)$ is the matrix of its eigenvalues and $\Lambda'=\mathbf{I}_N-\Lambda$.

Proof: It can be seen that: 1) $\|\mathbf{G}_t\|_p \le 1$, where $\|\mathbf{A}\|_p = \sup_{x\neq 0} \frac{\|\mathbf{A}x\|_p}{\|x\|_p}$ is matrix p-norm, defined in [45]; 2) there is a nonsingular $\mathbf{V} \in \Re^{n\times n}$ such that $\mathbf{V}\mathbf{G}_t\mathbf{V}^{-1} = \mathrm{diag}(\lambda_1, \lambda_2, \cdots, \lambda_N)$, therefore, the matrix of $\mathbf{G}_t$ is diagonalizable as defined in [45]. Thus, $\mathbf{G}_t = \mathbf{V}\Lambda\mathbf{V}^{-1}$. Also, it has been shown that for every symmetric matrix of $\mathbf{G}_t$ with eigenvalues of λ_m's, $(\mathbf{G}_t)^i = \mathbf{V}\Lambda^i\mathbf{V}^{-1}$, and $\mathrm{eig}(\mathbf{I}_N - \mathbf{G}_t) = 1-\lambda_m$ with $\lambda_m \in \mathbb{R}$. $\mathbf{G}_t$. Hence, proof is complete. □

Therefore, (27) can be rewritten as

$$\begin{aligned}\tilde{\mathbf{e}}_{\mathbf{A}}^{ik} &= -\mathbf{V}\Lambda'^{i+1}\mathbf{V}^{-1}\mathbf{F}_N^H\hat{\mathbf{s}}_{\mathbf{A}}^k\\ &= -\mathbf{V}\mathrm{diag}\left((1-\lambda_1)^{i+1},\ (1-\lambda_2)^{i+1},\ \ldots,\ (1-\lambda_N)^{i+1}\right)\\ &\quad\times \mathbf{V}^{-1}\mathbf{F}_N^H\hat{\mathbf{s}}_{\mathbf{A}}^k. \end{aligned} \tag{29}$$

From equations (27) and (29) it is obvious that the convergence of the algorithm is equivalent to the convergence of

$$\begin{aligned}&\lim_{i\to\infty} (\mathbf{I}_N - \mathbf{G}_t)^{i+1}\\ &= \mathbf{V}\,\mathrm{diag}\left((1-\lambda_1)^{i+1},\ (1-\lambda_2)^{i+1},\ \ldots,\ (1-\lambda_N)^{i+1}\right)_{i\to\infty}\mathbf{V}^{-1}.\end{aligned} \tag{30}$$

To assure convergence, it is required that $|1-\lambda_m| \le 1$. In summary, we should have for convergence,

$$\forall m : -1 \le 1-\lambda_m \le 1 \Rightarrow 0 \le \lambda_m \le 2 \Leftrightarrow \text{convergence}. \tag{31}$$

Above condition is fulfilled for $\mathbf{G}_t$, because $\mathbf{G}_t = \mathrm{diag}(g_{t1}, \ldots, g_{tN})$, $g_{tm} \in \{0, 1\}$ is diagonal with 0 and 1 entries on its diagonal and hence its eigenvalues are $\lambda_m \in \{0, 1\}$. Thus, it proves that the iterative method converges.

Appendix C
Proof of the Equation (9)

Proof: From (6):

$$\begin{aligned}\tilde{\mathbf{s}}_{\mathbf{A}}^{0k} &= \mathbf{G}_t\mathbf{F}_N^H\hat{\mathbf{s}}_{\mathbf{A}}^{\mathbf{k}}\\ \tilde{\mathbf{s}}_{\mathbf{A}}^{1k} &= \mathbf{G}_t(2\mathbf{I}_N - \mathbf{G}_t)\mathbf{F}_N^H\hat{\mathbf{s}}_A^k\\ \tilde{\mathbf{s}}_{\mathbf{A}}^{2k} &= [\mathbf{G}_t + \mathbf{G}_t(2\mathbf{I}_N - \mathbf{G}_t)(\mathbf{I}_N - \mathbf{G}_t)]\,\mathbf{F}_N^H\hat{\mathbf{s}}_{\mathbf{A}}^{\mathbf{k}}\\ \tilde{\mathbf{s}}_{\mathbf{A}}^{3k} &= \left[\mathbf{G}_t + \mathbf{G}_t(\mathbf{I}_N-\mathbf{G}_t) + \mathbf{G}_t(2\mathbf{I}_N-\mathbf{G}_t)(\mathbf{I}_N-\mathbf{G}_t)^2\right]\mathbf{F}_N^H\hat{\mathbf{s}}_{\mathbf{A}}^{\mathbf{k}}\\ &\ \ \vdots\end{aligned}$$

$$\begin{cases}\tilde{\mathbf{s}}_{\mathbf{A}}^{ik} = \left[\mathbf{G}_t + \mathbf{G}_t\sum\limits_{l=1}^{i-2}(\mathbf{I}_N-\mathbf{G}_t)^l + \mathbf{G}_t(2\mathbf{I}_N-\mathbf{G}_t)(\mathbf{I}_N-\mathbf{G}_t)^{i-1}\right]\\ \qquad\times\mathbf{F}_N^H\hat{\mathbf{s}}_{\mathbf{A}}^{\mathbf{k}}\\ (\mathbf{I}_N - \mathbf{G}_t)^i = \mathbf{0}, \quad i < 0\end{cases} \tag{32}$$

Hence, from $\sum_{l=1}^{i-2}(\mathbf{I}_N - \mathbf{G}_t)^l = \frac{(\mathbf{I}_N-\mathbf{G}_t)-(\mathbf{I}_N-\mathbf{G}_t)^{i-1}}{\mathbf{G}_t}$ we have:

$$\begin{aligned}&\tilde{\mathbf{s}}_{\mathbf{A}}^{ik}\\ &= \left[\mathbf{G}_t + (\mathbf{I}_N-\mathbf{G}_t) - (\mathbf{I}_N-\mathbf{G}_t)^{i-1} + \mathbf{G}_t(2\mathbf{I}_N-\mathbf{G}_t)(\mathbf{I}_N-\mathbf{G}_t)^{i-1}\right]\\ &\quad\times\mathbf{F}_N^H\hat{\mathbf{s}}_{\mathbf{A}}^{\mathbf{k}}\\ &= \left[\mathbf{I}_N - (\mathbf{I}_N-\mathbf{G}_t)^{i-1} + \mathbf{G}_t(2\mathbf{I}_N-\mathbf{G}_t)(\mathbf{I}_N-\mathbf{G}_t)^{i-1}\right]\mathbf{F}_N^H\hat{\mathbf{s}}_{\mathbf{A}}^{\mathbf{k}}\\ &= \left[(\mathbf{I}_N-\mathbf{G}_t)^{i-1}\left(2\mathbf{G}_t - \mathbf{G}_t{}^2 - \mathbf{I}_N\right) + \mathbf{I}_N\right]\mathbf{F}_N^H\hat{\mathbf{s}}_{\mathbf{A}}^{\mathbf{k}}\\ &= \left[-(\mathbf{I}_N-\mathbf{G}_t)^{i-1}(\mathbf{I}_N-\mathbf{G}_t)^2 + \mathbf{I}_N\right]\mathbf{F}_N^H\hat{\mathbf{s}}_{\mathbf{A}}^{\mathbf{k}}\\ &= \left[\mathbf{I}_N - (\mathbf{I}_N-\mathbf{G}_t)^{i+1}\right]\mathbf{F}_N^H\hat{\mathbf{s}}_{\mathbf{A}}^{\mathbf{k}}\\ &= \left[\mathbf{I}_N - (\mathbf{I}_N-\mathbf{G}_t)^{i+1}\right]\mathbf{F}_N^H(\mathbf{G}_f\mathbf{c}_{\mathbf{A}}'^{\mathbf{k}} + \mathbf{D}_{\mathbf{AB}}^{-1}\mathbf{F}_N\nu_{\mathbf{AB}})\\ &= \left[\mathbf{I}_N - (\mathbf{I}_N-\mathbf{G}_t)^{i+1}\right](\mathbf{G}_t\mathbf{F}_N^H\mathbf{c}_{\mathbf{A}}'^{\mathbf{k}} + \mathbf{F}_N^H\mathbf{D}_{\mathbf{AB}}^{-1}\mathbf{F}_N\nu_{\mathbf{AB}}),\\ &\qquad for\ i > 0\end{aligned} \tag{33}$$

By taking $N-$point FFT for transforming from time domain to frequency domain the proof is complete. □

Appendix D
Proof of the Equation (13) for Infinite Number of Iteration

Proof:

$$\begin{cases}\tilde{\mathbf{s}}_{\mathbf{A}}^{ik} = \widetilde{\Psi}_{\mathbf{A}} + \left(\mathbf{I}_N - \widetilde{\mathbf{G}}_t\right)\tilde{\mathbf{s}}_{\mathbf{A}}^{(i-1)k} & i > 0\\ \tilde{\mathbf{s}}_{\mathbf{A}}^{0k} = \widetilde{\Psi}_{\mathbf{A}} & i = 0,\end{cases} \tag{34}$$

where $\widetilde{\Psi}_{\mathbf{A}} = \mathbf{F}_N^H\mathbf{E}\mathbf{F}_N\Psi_{\mathbf{A}}$ and $\widetilde{\mathbf{G}}_t = \mathbf{F}_N^H\mathbf{E}\mathbf{F}_N\mathbf{G}_t$ are low pass filtered version of $\Psi_{\mathbf{A}}$ and $\mathbf{G}_t$, respectively.

At the infinity of iteration $\tilde{\mathbf{s}}_{\mathbf{A}}^{\infty k} = \widetilde{\mathbf{G}}_t^{\dagger}\tilde{\mathbf{s}}_{\mathbf{A}}^{0k}$. Hence

$$\tilde{\mathbf{s}}_{\mathbf{A}}^{\infty k} = (\mathbf{F}_N^H\mathbf{E}\mathbf{F}_N\mathbf{G}_t)^{\dagger}\mathbf{F}_N^H\mathbf{E}\mathbf{G}_f\hat{\mathbf{s}}_{\mathbf{A}}^{\mathbf{k}}.$$

But, $\mathbf{G}_t = \mathbf{F}_N^H\mathbf{G}_f\mathbf{F}_N$

$$\begin{aligned}\tilde{\mathbf{s}}_{\mathbf{A}}^{\infty k} &= (\mathbf{F}_N^H\mathbf{E}\mathbf{G}_f\mathbf{F}_N)^{\dagger}\mathbf{F}_N^H\mathbf{E}\mathbf{G}_f\ (\mathbf{G}_f\mathbf{c}'^{\mathbf{k}}_{\mathbf{A}} + \mathbf{D}_{\mathbf{AB}}^{-1}\mathbf{F}_N\nu_{\mathbf{AB}})\\ &= \mathbf{F}_N^H\mathbf{G}_f^{\dagger}\mathbf{E}^{\dagger}\mathbf{F}_N\mathbf{F}_N^H\mathbf{E}\mathbf{G}_f\mathbf{c}'^{\mathbf{k}}_{\mathbf{A}}\\ &\quad + \mathbf{F}_N^H\mathbf{G}_f^{\dagger}\mathbf{E}^{\dagger}\mathbf{F}_N\mathbf{F}_N^H\mathbf{E}\mathbf{G}_f\mathbf{A}\mathbf{B}^{-1}\mathbf{F}_N\nu_{\mathbf{AB}}\\ &= \mathbf{F}_N^H\mathbf{c}'^{\mathbf{k}}_{\mathbf{A}} + \mathbf{F}_N^H\mathbf{A}\mathbf{B}^{-1}\mathbf{F}_N\nu_{\mathbf{AB}}.\end{aligned}$$

By applying the $N-$point FFT at the ending stage of Fig. 2 for convergent iterative receiver the relationship is proved. □

References

[1] E. Yaacoub, F. Filali, and A. Abu-Dayya, "QoE enhancement of SVC video streaming over vehicular networks using cooperative LTE/802.11p communications," *IEEE J. Sel. Topics Signal Process.*, vol. 9, no. 1, pp. 37–49, Feb. 2015.

[2] M. Zhao, X. Wang, Y. Liu, and S. Feng, "Sparse beamforming in multiple multi-antenna amplify-and-forward relay networks," *IEEE Commun. Lett.*, vol. 18, no. 6, pp. 1023–1026, Jun. 2014.

[3] Q. Z. Ahmed, S. Ahmed, M.-S. Alouini, and S. Aïssa, "Minimizing the symbol-error-rate for amplify-and-forward relaying systems using evolutionary algorithms," *IEEE Trans. Commun.*, vol. 63, no. 2, pp. 390–400, Feb. 2015.

[4] H.-B. Kong, C. Song, H. Park, and I. Lee, "A new beamforming design for MIMO AF relaying systems with direct link," *IEEE Trans. Commun.*, vol. 62, no. 7, pp. 2286–2295, Jul. 2014.

[5] S. Zhao and W. Chen, "To code or not to code: Maximizing the achievable rate region of two-way decode-and-forward multiantenna relay channel," *IEEE Commun. Lett.*, vol. 18, no. 8, pp. 1303–1306, Aug. 2014.

[6] N. Varshney, A. V. Krishna, and A. K. Jagannatham, "Selective DF protocol for MIMO STBC based single/multiple relay cooperative communication: End-to-end performance and optimal power allocation," *IEEE Trans. Commun.*, vol. 63, no. 7, pp. 2458–2474, Jul. 2015.

[7] Q. F. Zhou, W. H. Mow, S. Zhang, and D. Toumpakaris, "Two-way decode-and-forward for low-complexity wireless relaying: Selective forwarding versus one-bit soft forwarding," *IEEE Trans. Wireless Commun.*, vol. 15, no. 3, pp. 1866–1880, Mar. 2016.

[8] E. S. Lo and K. B. Letaief, "Cooperative concatenated coding for improved distance spectrum and diversity in wireless systems," *IEEE Trans. Commun.*, vol. 59, no. 2, pp. 382–387, Feb. 2011.

[9] Y. Fang, Y. L. Guan, G. Bi, L. Wang, and F. C. M. Lau, "Rate-compatible root-protograph LDPC codes for quasi-static fading relay channels," *IEEE Trans. Veh. Technol.*, vol. 65, no. 4, pp. 2741–2747, Apr. 2016.

[10] A. Nosratinia, T. E. Hunter, and A. Hedayat, "Cooperative communication in wireless networks," *IEEE Commun. Mag.*, vol. 42, no. 10, pp. 74–80, Oct. 2004.

[11] A. Karbalayghareh, M. Nasiri-Kenari, and M. Hejazi, "Convolutional network-coded cooperation in multi-source networks with a multi-antenna relay," *IEEE Trans. Wireless Commun.*, vol. 13, no. 8, pp. 4323–4333, Aug. 2014.

[12] W.-M. Lai, Y.-M. Chen, and Y.-L. Ueng, "Raptor-coded noncoherent cooperative schemes based on distributed unitary space–time modulation," *IEEE Trans. Commun.*, vol. 63, no. 8, pp. 2873–2884, Aug. 2015.

[13] H. Sun, S. X. Ng, C. Dong, and L. Hanzo, "Decode-and-forward cooperation-aided triple-layer turbo-trellis-coded hierarchical modulation," *IEEE Trans. Commun.*, vol. 63, no. 4, pp. 1136–1148, Apr. 2015.

[14] S. Schwandter, A. G. I. Amat, and G. Matz, "Spatially-coupled LDPC codes for decode-and-forward relaying of two correlated sources over the BEC," *IEEE Trans. Commun.*, vol. 62, no. 4, pp. 1324–1337, Apr. 2014.

[15] X. Lu, J. Li, and Y. Liu, "New soft-encoding relay (SoER) mechanisms for wireless relay systems: Convolutional and turbo constructions," *IEEE Trans. Wireless Commun.*, vol. 15, no. 4, pp. 2443–2457, Apr. 2016.

[16] E. G. Larsson and B. R. Vojcic, "Cooperative transmit diversity based on superposition modulation," *IEEE Commun. Lett.*, vol. 9, no. 9, pp. 778–780, Sep. 2005.

[17] A. P. Millar, S. Weiss, and R. W. Stewart, "Training-based channel estimation algorithms for dual hop MIMO OFDM relay systems," *IEEE Trans. Commun.*, vol. 63, no. 12, pp. 4711–4726, Dec. 2015.

[18] D. Qin and Y. Wang, "BER minimization for AF relay-assisted OFDM systems," *IEEE Commun. Lett.*, vol. 19, no. 3, pp. 495–498, Mar. 2015.

[19] B. Zhang, J. Hu, Y. Huang, M. El-Hajjar, and L. Hanzo, "Outage analysis of superposition-modulation-aided network-coded cooperation in the presence of network coding noise," *IEEE Trans. Veh. Technol.*, vol. 64, no. 2, pp. 493–501, Feb. 2015.

[20] X. Jin and H.-N. Kim, "Switched-power two-layer superposition coding in cooperative decode-forward relay systems," *IEEE Trans. Wireless Commun.*, vol. 15, no. 3, pp. 2193–2204, Mar. 2016.

[21] X. Lu, J. Li, and Y. Liu, "Cooperative transmission through signal-superposition-based braid coding," *IEEE Trans. Veh. Technol.*, vol. 65, no. 5, pp. 3100–3114, May 2016.

[22] S.-W. Ko, J.-H. Kim, J.-S. Yoon, and H.-K. Song, "Cooperative OFDM system for high throughput in wireless personal area networks," *IEEE Trans. Consum. Electron.*, vol. 56, no. 2, pp. 458–462, May 2010.

[23] A. Rahmati and P. Azmi, "Coded cooperation diversity for uncoded oversampled OFDM systems," *Signal Process.*, vol. 89, no. 7, pp. 1370–1378, Jul. 2009.

[24] E. Balevi and A. Ö. Yilmaz, "Analysis of frequency domain oversampled MMSE SC-FDE," *IEEE Commun. Lett.*, vol. 20, no. 2, pp. 232–235, Feb. 2016.

[25] M. Ma, X. Huang, B. Jiao, and Y. J. Guo, "Optimal orthogonal precoding for power leakage suppression in DFT-based systems," *IEEE Trans. Commun.*, vol. 59, no. 3, pp. 844–853, Mar. 2011.

[26] M.-J. Hao and C.-H. Lai, "Precoding for PAPR reduction of OFDM signals with minimum error probability," *IEEE Trans. Broadcast.*, vol. 56, no. 1, pp. 120–128, Mar. 2010.

[27] X. Huang, J. A. Zhang, and Y. J. Guo, "Out-of-band emission reduction and a unified framework for precoded OFDM," *IEEE Commun. Mag.*, vol. 53, no. 6, pp. 151–159, Jun. 2015.

[28] A. S. Bedi, J. Akhtar, K. Rajawat, and A. K. Jagannatham, "BER-optimized precoders for OFDM systems with insufficient cyclic prefix," *IEEE Commun. Lett.*, vol. 20, no. 2, pp. 280–283, Feb. 2016.

[29] H. Schulze and C. Lueders, *Theory and Applications of OFDM and CDMA: Wideband Wireless Communications*. New York, NY, USA: Wiley, 2005.

[30] R. AliHemmati and P. Azmi, "Iterative reconstruction-based method for clipping noise suppression in OFDM systems," *IEE Proc.-Commun.*, vol. 152, no. 4, pp. 452–456, Aug. 2005.

[31] T. E. Hunter and A. Nosratinia, "Diversity through coded cooperation," *IEEE Trans. Wireless Commun.*, vol. 5, no. 2, pp. 283–289, Feb. 2006.

[32] S. F. A. Shah and A. H. Tewfik, "Design and analysis of post-coded OFDM systems," *IEEE Trans. Wireless Commun.*, vol. 7, no. 12, pp. 4907–4918, Dec. 2008.

[33] Y.-P. Lin and S.-M. Phoong, "BER minimized OFDM systems with channel independent precoders," *IEEE Trans. Signal Process.*, vol. 51, no. 9, pp. 2369–2380, Sep. 2003.

[34] S. Xu, R. C. D. Lamare, and H. V. Poor, "Distributed compressed estimation based on compressive sensing," *IEEE Signal Process. Lett.*, vol. 22, no. 9, pp. 1311–1315, Sep. 2015.

[35] S.-C. Pei and S.-G. Huang, "Fast discrete linear canonical transform based on CM-CC-CM decomposition and FFT," *IEEE Trans. Signal Process.*, vol. 64, no. 4, pp. 855–866, Feb. 2016.

[36] Y. C. Eldar and T. Michaeli, "Beyond bandlimited sampling," *IEEE Signal Process. Mag.*, vol. 26, no. 3, pp. 48–68, May 2009.

[37] J. Wang, S. Kwon, P. Li, and B. Shim, "Recovery of sparse signals via generalized orthogonal matching pursuit: A new analysis," *IEEE Trans. Signal Process.*, vol. 64, no. 4, pp. 1076–1089, Feb. 2016.

[38] S. Ono and I. Yamada, "Signal recovery with certain involved convex data-fidelity constraints," *IEEE Trans. Signal Process.*, vol. 63, no. 22, pp. 6149–6163, Nov. 2015.

[39] M. A. Davenport and J. Romberg, "An overview of low-rank matrix recovery from incomplete observations," *IEEE J. Sel. Topics Signal Process.*, vol. 10, no. 4, pp. 608–622, Jun. 2016.

[40] C.-Z. Zhan, Y.-L. Chen, and A.-Y. Wu, "Iterative superlinear-convergence SVD beamforming algorithm and VLSI architecture for MIMO-OFDM systems," *IEEE Trans. Signal Process.*, vol. 60, no. 6, pp. 3264–3277, Jun. 2012.

[41] F. Marvasti, M. Analoui, and M. Gamshadzahi, "Recovery of signals from nonuniform samples using iterative methods," *IEEE Trans. Signal Process.*, vol. 39, no. 4, pp. 872–878, Apr. 1991.

[42] F. Marvasti, *Nonuniform Sampling Theory and Practice*. New York, NY, USA: Kluwer, 2001.

[43] J. G. Proakis, *Digital Communications*. New York, NY, USA: McGraw-Hill, 1995.

[44] S. Dang, J. P. Coon, and G. Chen, "An equivalence principle for OFDM-based combined bulk/per-subcarrier relay selection over equally spatially correlated channels," *IEEE Trans. Veh. Technol.*, vol. 66, no. 1, pp. 122–133, Jan. 2017.

[45] G. H. Golub and C. F. Van Loan, *Matrix Computations*. Baltimore, MD, USA: The Johns Hopkins Univ. Press, 1996.

Alireza Rahmati was born in Tehran, Iran. He received the B.Sc. degree in electrical engineering from the Sharif University of Technology, Tehran, Iran, in 2004, and the M.Sc. and Ph.D. degrees in telecommunication systems engineering from Tarbiat Modares University, Tehran, in 2007 and 2012, respectively. Currently, he is a Post-Doctoral Fellow with the Department of Electrical and Computer Engineering, Ryerson University, Toronto, Canada. From 2007 to 2015, he was with the Advanced Electronic and Communication Research Center, Tehran. His main research interests are statistical signal processing, navigation and positioning, 5G relay networks, and full-duplex radio.

Kaamran Raahemifar (S'91–M'99–SM'02) received the B.Sc. degree in electrical engineering from the Sharif University of Technology, Tehran, Iran, in 1988, the M.A.Sc. degree from the Electrical and Computer Engineering Department, Waterloo University, Waterloo, ON, Canada, in 1993, and the Ph.D. degree from Windsor University, ON, Canada, in 1999. He joined Ryerson University in 1999 and was tenured in 2001. Since 2011, he has been a Professor with the Department of Electrical and Computer Engineering, Ryerson University. His research interests include VLSI circuit simulation, design and testing, signal processing, and hardware implementation of biomedical signals. He was the recipient of the ELCE-GSA Professor of the Year Award (Elected by Graduate Student's Body, 2010), the Faculty of Engineering, Architecture, and Science Best Teaching Award in 2011, the Department of Electrical and Computer Engineering Best Teaching Award in 2011, and the Research Award in 2014. He has been a recipient for more than U.S. \$6 million external research funds during his time at Ryerson.

Alagan Anpalagan (M'02–SM'06) received the B.A.Sc., M.A.Sc., and Ph.D. degrees in electrical engineering from the University of Toronto. He is currently a Professor with the Department of Electrical and Computer Engineering, Ryerson University, where he directs a research group working on radio resource management and radio access and networking areas within the WINCORE Laboratory. He co-authored three edited books, *Design and Deployment of Small Cell Networks* (Cambridge University Press, 2014), *Routing in Opportunistic Networks* (Springer, 2013), and *Handbook on Green Information and Communication Systems* (Academic Press, 2012). He is a registered Professional Engineer in the province of Ontario, Canada, and a fellow of the Institution of Engineering and Technology. He was the recipient of the Dean's Teaching Award in 2011, the Faculty Scholastic, Research and Creativity Award in 2010, 2014, and 2017, and the Faculty Service Award in 2011 and 2013 in Ryerson University. He also received the Exemplary Editor Award from the IEEE ComSoc in 2013 and the Editor-in-Chief Top10 Choice Award for the *Transactions on Emerging Telecommunications Technology* in 2012. He currently serves as the TPC Vice-Chair of the IEEE VTC Fall-2017. He served as the TPC Co-Chair of the IEEE Globecom'15: SAC Green Communication and Computing, the IEEE WPMC'12 Wireless Networks, the IEEE PIMRC'11 Cognitive Radio and Spectrum Management, and the IEEE CCECE'04/08. He has been serving as the Vice Chair of the IEEE SIG on Green and Sustainable Networking and Computing with Cognition and Cooperation since 2015. He served as the IEEE Canada Central Area Chair from 2012 to 2014, the IEEE Toronto Section Chair from 2006 to 2007, the ComSoc Toronto Chapter Chair from 2004 to 2005, and the IEEE Canada Professional Activities Committee Chair from 2009 to 2011. He served as an Editor of the IEEE COMMUNICATIONS SURVEYS AND TUTORIALS from 2012 to 2014, the IEEE COMMUNICATIONS LETTERS from 2010 to 2013, *Wireless Personal Communications* from 2011 to 2013, and the EURASIP JOURNAL OF WIRELESS COMMUNICATIONS AND NETWORKING from 2004 to 2009.

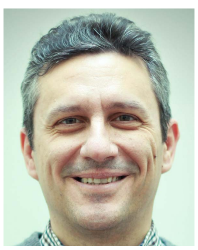

Theodoros A. Tsiftsis (S'02–M'04–SM'10) was born in Lamia, Greece, in 1970. He received the B.Sc. degree in physics from the Aristotle University of Thessaloniki, Greece, in 1993, the M.Sc. degree in digital systems engineering from the Heriot-Watt University, Edinburgh, U.K., in 1995, the M.Sc. degree in decision sciences from the Athens University of Economics and Business, in 2000, and the Ph.D. degree in electrical engineering from the University of Patras, Greece, in 2006. He joined the Technological Educational Institute of Central Greece, in 2010. He is currently an Associate Professor in communication technologies with the School of Engineering, Nazarbayev University, Astana, Kazakhstan. He has authored or co-authored over 120 technical papers in scientific journals and international conferences. His research interests include the broad areas of cooperative communications, cognitive radio, communication theory, wireless powered communication systems, and optical wireless communication systems. He acts as a reviewer for several international journals and conferences. He has served as a Senior Editor or an Associate Editor in the Editorial Boards of the IEEE TRANSACTIONS ON VEHICULAR TECHNOLOGY and the IEEE COMMUNICATIONS LETTERS. He is currently an Area Editor for Wireless Communications II of the IEEE TRANSACTIONS ON COMMUNICATIONS and an Associate Editor of the IEEE TRANSACTIONS ON MOBILE COMPUTING.

Paeiz Azmi (M'09–SM'10) was born in Tehran, Iran, in 1974. He received the B.Sc., M.Sc., and Ph.D. degrees in electrical engineering from the Sharif University of Technology, Tehran, in 1996, 1998, and 2002, respectively. From 1999 to 2001, he was with the Advanced Communication Science Research Laboratory, Iran Telecommunication Research Center (ITRC), Tehran. Since 2002, he has been with the Electrical and Computer Engineering Department, Tarbiat Modares University, Tehran, where he became an Associate Professor in 2006 and he is currently a Full Professor. From 2002 to 2005, he was with the Signal Processing Research Group, ITRC. His current research interests include modulation and coding techniques, digital signal processing, wireless communications, and estimation and detection theories.

Nikolaos I. Miridakis was born in Athens, Greece, in 1982. He received the M.Sc. degree in networking and data communications from the Department of Information Systems, Kingston University, U.K., in 2008, and the Ph.D. degree in networking and data communications from the Department of Informatics, University of Piraeus, Greece, in 2012. Since 2007, he has been with the Department of Computer Engineering, Piraeus University of Applied Sciences, Greece, where he is currently an Adjunct Lecturer and a Research Associate. Also, since 2012, he has been with the Department of Informatics, University of Piraeus, where he is currently a Senior Research Associate. His research interests include wireless communications, and more specifically interference analysis and management in wireless communications, multicarrier communications, MIMO systems, statistical signal processing, diversity reception, fading channels, and cooperative communications.

Dr. Miridakis serves as a reviewer and a TPC member for several prestigious international journals and conferences.